journal

J. Am. Ceram. Soc., 86 [7] 1182–89 (2003)

Structure Sensitivity of Photochemical Oxidation and Reduction Reactions on $SrTiO_3$ Surfaces

Jennifer L. Giocondi and Gregory S. Rohrer*,†

Department of Materials Science and Engineering, Carnegie Mellon University, Pittsburgh, Pennsylvania 15213-3890

The photochemical reduction of Ag^+ and oxidation of Pb^{2+} from aqueous solution by $SrTiO_3$ leave insoluble reaction products (silver and PbO_2, respectively) on the surface. Microscopic analysis has been used to relate the rates of these two reactions to the structure and orientation of $SrTiO_3$ surfaces. The nonpolar (100) surface is the most reactive for silver reduction and the composition of the termination layer does not influence this reaction. On the polar (111) surface, the reduction and oxidation reactions occur on terraces with different terminations and opposite charges; this leads to a nonuniform distribution of reaction products. The polar (110) surface is the least reactive, and the majority of the reaction products are observed at steps along <100> directions where the more reactive {100} surfaces are exposed. The distribution of oxidation products found on (110) terraces is also influenced by the composition and charge of the surface termination. The results show that the photochemical reactivity of $SrTiO_3$ is anisotropic and that, on polar surfaces, dipolar fields arising from charged surface domains influence the transport of photogenerated charge carriers and promote spatially selective oxidation and reduction reactions.

I. Introduction

During a heterogeneous photochemical reaction, photogenerated electrons and holes migrate to the solid surface where they can participate in reactions with adsorbed species. When these reactions occur on the surface of an oxide pigment particle embedded in a composite, the stability of the system is usually compromised.[1,2] Therefore, pigment particles are modified to minimize photochemical reaction rates.[3] However, there are also a number of applications for photochemically active ceramics where it is desirable to maximize the efficiency of photon stimulated reactions. Photochemical air and water purifiers,[4–6] self-cleaning surface treatments,[7] and water photolysis catalysts[8,9] are examples. For these high-reactivity applications, an incomplete knowledge of structure-property relationships limits the search for improved materials.

As a starting point for developing a useful structure property relation, we note that the photochemical properties of some transition metal oxides are known to be surface structure sensitive.[10–13] In other words, their reactivity depends not only on the chemical composition, but also on the orientation of the surface and the defect structure. The mechanisms underpinning the surface structure sensitivity of reactivity are not yet well understood. Recent observations of photochemical reactions on $BaTiO_3$ surfaces indicate that internal dipolar fields can drive photogenerated electrons and holes to different locations of the surface, and this leads to a spatial separation of the reduction and oxidation products.[12,13] If this spatial separation of charge carriers and reaction products reduces both the rate of electron-hole recombination and the rate of the back reaction of the reduced and oxidized species, then it is a potentially important mechanism for increasing the efficiency of photochemically active ceramics.

In $BaTiO_3$, internal dipolar fields arise from the spontaneous polarization of its ferroelectric domains. However, dipolar fields can also arise from defect segregation[14] or polar surface terminations.[15] The purpose of the current paper is to describe the structure sensitivity of photochemical reactions on the surfaces of $SrTiO_3$, which is nearly isostructural with $BaTiO_3$, but not ferroelectric. We have found that the photochemical reactivity of the surface depends on orientation and that, for polar surface orientations, the composition and charge of the surface termination layer strongly influence the photochemical reactivity. Furthermore, we interpret the spatially selective reactivity on the polar surfaces of $SrTiO_3$ as evidence that polar surface domains can effectively separate photogenerated charge carriers by a mechanism similar to that in $BaTiO_3$, but without the presence of ferroelectric polarizations.

II. Experimental Procedures

The experimental approach is based on the use of photochemical "probe" reactions that leave insoluble products on the surface at the sites of oxidation and reduction. The locations of the reaction sites are determined by examining the surfaces before and after the probe photochemical reaction using atomic force microscopy (AFM). Polycrystals were used to examine the activity over the range of all crystallographic orientations, and single crystals were used to examine the activity of specific orientations in greater detail. Details of the sample preparation and photochemical reactions are given below.

Polycrystalline $SrTiO_3$ ceramics were formed by uniaxially compacting commercially available powder (99.5%, Alfa Aeasar, Ward Hill, MA) under 150 MPa to form disk-shaped pellets with a thickness of 3 mm and an approximate diameter of 11 mm. The pellets were then placed in an alumina crucible with an excess of the parent powder to ensure that the pellet did not contact the crucible. The samples were heated to 900°C (all ramp rates were 5°C/min) for 12 h in air to burn off any residual organics, sintered for 12 h at 1360°C, and the grains were grown for 3 h at 1470°C to achieve an average grain size of 25 μm. At the end of the grain growth step, the samples cooled in the furnace. The sintered samples were then lapped flat using a 9 μm Al_2O_3 (Buehler, Lake Bluff, IL) aqueous solution and polished with a basic 0.02 μm colloidal silica solution (Buehler). Polished samples were annealed in air at 1200°C for 6 h to remove polishing damage, facet the surface, and thermally etch the grain boundaries.

Mechano-chemically polished (100)-, (110)-, and (111)-oriented $SrTiO_3$ single crystals were obtained from Crystal GmbH

D. Bonnell—contributing editor

Manuscript No. 186570. Received November 14, 2002; approved January 20, 2003.

This work was supported by the National Science Foundation under grant DMR 0072151.

*Member, American Ceramic Society.

†Corresponding author.

(Berlin, Germany). The as-received crystals were annealed at 1200°C in air for 6 h before any of the experiments described below.

We use the reduction of Ag^+ by photogenerated electrons[16,17] and the oxidation of Pb^{2+} by photogenerated holes[18,19] to create insoluble products that mark the locations of the reactions described below:

$$Ag^+ + e^- = Ag \quad (1)$$

$$Pb^{2+} + 2H_2O + 2h^+ = PbO_2 + 4H^+ \quad (2)$$

The photochemical reactions were conducted in the following way: a 1.7-mm-thick viton O-ring was placed on the sample surface and the interior volume was filled with a solution containing a dissolved metal salt (0.115*M* aqueous $AgNO_3$ (Fisher Scientific, Pittsburgh, PA) or 0.0115*M* aqueous $Pb(C_2H_3O_2)_2$ (Fisher Scientific). A 0.2-mm-thick quartz coverslip was then placed on top of the O-ring and held in place by the surface tension of the solution. The sample was illuminated using a 300 W mercury lamp. The exposure times were 3 s and 150 s for the silver reduction and the lead oxidation, respectively. After exposure, the sample was rinsed with deionized H_2O, dried with forced air, and then imaged using atomic force microscopy (AFM). In the case of experiments done with single crystals, individual sets of (100)-, (110)-, and (111)-oriented crystals were illuminated simultaneously, during a single exposure, for both reactions. In control experiments conducted with light made up of energies less than strontium titanate's band gap, no photochemical reactions were observed.

The surface topography of all specimens was observed using AFM (Park Scientific Instruments, Sunnyvale, CA) both before and after the probe reactions. In this way, reaction products could be differentiated from pre-existing surface features. Gold-coated, sharpened pyramidal Si_3N_4 probes (Model ML06A-F, Thermomicroscopes, Sunnyvale, CA) were used for images obtained in contact mode. The force varied between 0.25 nN and 10 nN, with the lowest contact forces being used after the reaction and the higher forces before the reaction. In most cases, the reaction products were immobile and not significantly changed during imaging with low-contact force. However, in cases where the probe interacted with the deposits, noncontact AFM (NC-AFM) was used. Conical silicon probes (Model UL20C/D, Thermomicroscopes) with resonant frequencies of ~360kHz were used for NC-AFM imaging. Most topographs presented here are displayed in grayscale; light contrast indicates relatively high regions of the surface, and dark contrast indicates relatively low areas of the surface. Step heights are measured by subtracting the mean vertical position of the pixels on the lower terrace from the mean vertical position of the pixels on the upper terrace. The standard deviation of such measurements is 0.2 Å.

After the AFM imaging was completed, the crystallographic orientations of individual grains in a polycrystalline sample were determined from electron backscattered diffraction patterns (EBSP). An EBSP was collected for 75 grains and the patterns were indexed using orientation imaging microscopy software (version 2.6, TexSEM Laboratories, Provo, UT). The software returns a set of Euler angles (ϕ_1, Φ, ϕ_2) for each grain, which are used to specify a relationship between the sample reference frame and the crystallographic axes. From these data, the components of the surface normals can be computed.

Laue backscattered X-ray diffraction patterns were obtained for the $SrTiO_3$ single crystals. Experimental patterns were compared with simulated patterns from the commercial software Desktop Microscopist (Virtual Labs, Ukiah, CA). These diffraction patterns were used to confirm the surface orientation of the crystals and to determine the in-plane orientations of surface features observed by AFM.

Energy dispersive X-ray (EDX) spectroscopy (Link ISIS, Oxford Instruments, Buckinghamshire, England) conducted via scanning electron microscopy (Model XL30FEG, Phillips, Eindhoven, The Netherlands) was used to analyze the elemental composition of the solids deposited during the photochemical reaction. It was confirmed that the deposits from the silver reduction reaction contained silver and that deposits from the lead oxidation reaction contained lead. Attempts to determine the phase of the deposits using X-ray diffraction were unsuccessful.

III. Results

The topographic AFM images in Fig. 1 show the surfaces of two representative grains of a $SrTiO_3$ polycrystal after the photochemical reduction of silver. Both images show circular features superimposed on a semiregular facet structure. Because the facets are present in the same configuration before the reduction reaction, we conclude that the circular features that appear after the reaction

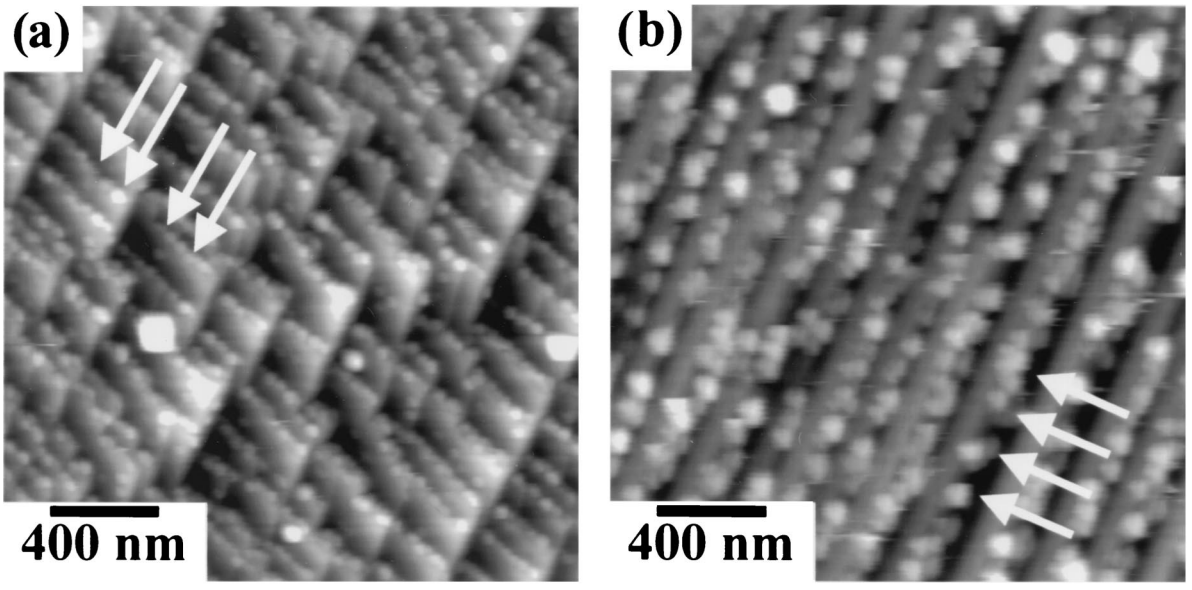

Fig. 1. Topographic AFM images of the surfaces of crystallites in a $SrTiO_3$ polycrystal after illumination in $AgNO_3$ solution. Silver (white contrast) deposits selectively on only some facets as indicated by the arrows. (a) surface composed of three types of facets with only one facet type active for silver reduction; (b) surface composed of two types of facets with only one facet type active for silver reduction. The vertical black-to-white contrast in (a) and (b) are 300 nm and 150 nm, respectively.

contain reduced silver. The image in Fig. 1(a) shows that while the surface is bounded by three facets, the majority of the silver has accumulated on only one of the facets (as indicated by the arrows on the image). The surface shown in Fig. 1(b) is bound by two types of facets that form a stair-step structure and, again, only the facet indicated by the arrows accumulated silver.

Using the EBSP data, it is possible to specify the crystal orientation. However, the facets that actually bound the surface are inclined with respect to the average measured orientation. When this inclination can be measured from the AFM topographs, it is possible to index the surface facets. However, this is not always possible. Because of tip convolution effects, accurate measurements of the inclination are feasible only when the area of the facet is relatively large (greater than a few hundred square nanometers). For example, in Fig. 1, the very narrow facets where the silver is accumulated cannot be indexed with any degree of certainty. However, based on the facets that can be reliably indexed, we conclude that surfaces within 24° of the {100} plane remain flat, whereas surfaces with any other orientation are bound by some combination of the following three planes: {110}, {111}, and a complex facet inclined ~24° from {100}. Among these three surfaces, those near {100} accumulated more silver than the other two. With this limited set of orientations identified, further studies of the orientation dependence of the photochemical activity were conducted exclusively on single crystals with the three low index orientations.

The topograph in Fig. 2(a) shows an annealed (100)-oriented $SrTiO_3$ single crystal. The surface consists of (100) terraces with step edges whose orientations are determined by the local miscut. Based on the stacking of atomic planes parallel to (100), the heights of all possible steps are equal to $(N/2)d_{100}$, where N is an integer, d_{100} is the spacing between (100) planes, and the smallest possible step has $N = 1$. Because the crystal can be terminated by a TiO_2 or SrO plane, we can distinguish odd-N steps, which change the termination, from even-N steps, which preserve the termination (see Fig. 3). Although the current data does not allow us to determine which terrace has which termination, the mixture of even- and odd-N steps allows us to be certain that both terminations are simultaneously present on this surface. The observation of mixed terminations is consistent with earlier studies of this surface.[20]

The topograph in Fig. 2(b) shows the surface after illumination in the presence of aqueous $AgNO_3$. After this treatment, it is no longer possible to identify individual steps and the entire surface is uniformly covered with silver deposits. The lead oxidation reaction was performed on another crystal prepared in the same way and the result is illustrated in Fig. 2(c). In this case, the lead oxide deposits (isolated white contrast) are found only on widely spaced,

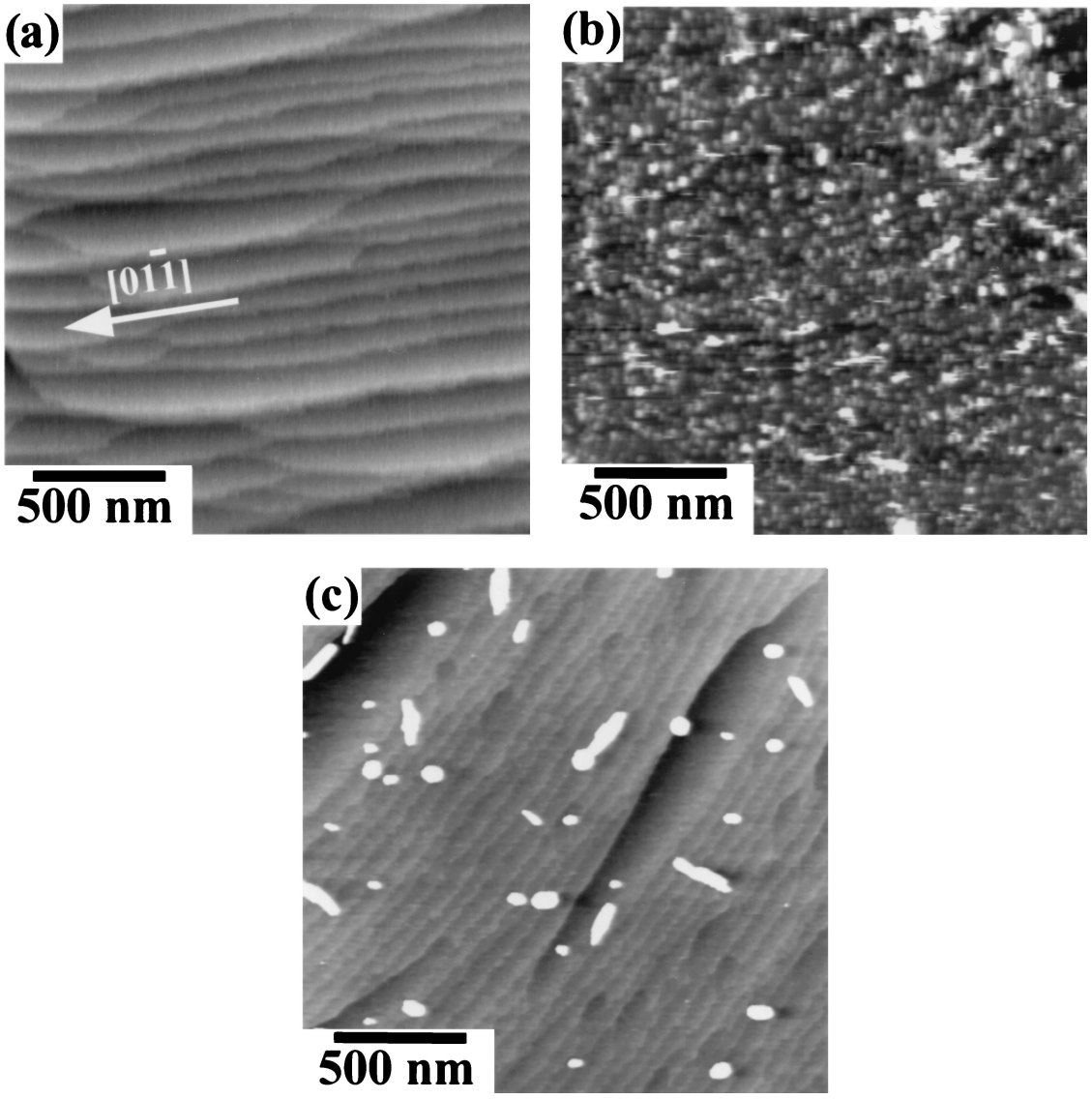

Fig. 2. Topographic AFM images of the surfaces of (100) -oriented $SrTiO_3$ single crystals. (a) Before the reactions. (b) The same surface after illumination in an aqueous $AgNO_3$ solution. The white contrast corresponds to silver. (c) A different surface after illumination in an aqueous lead acetate solution. The white contrast corresponds to lead oxide deposits. The ranges of the vertical black-to-white contrast in (a) to (c) are 25 nm, 100 nm, and 25 nm, respectively.

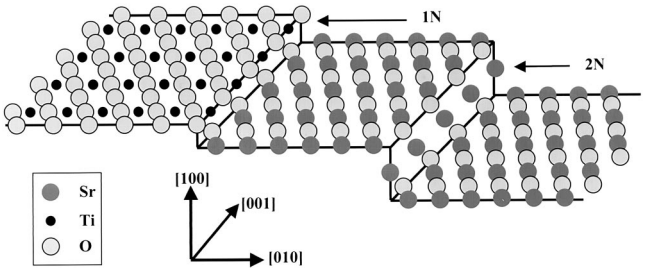

Fig. 3. Schematic drawing of the possible $SrTiO_3$ (100) surface terminations. The left terrace has a TiO_2 termination. Traversing an odd-*N* step changes the termination to SrO (middle terrace) while traversing an even-*N* step does not change the chemical termination (right terrace). Layer spacing (N) = 1/2a = 1.95 Å.

localized regions of the surface. For both the reduction and oxidation reactions on the {100} surface, there is no obvious correlation between the reactivity and terrace composition.

The topograph in Fig. 4(a) shows the surface of an annealed $SrTiO_3$ (111) surface. Adjacent (111) terraces are separated by a combination of straight and curved steps. The straight steps are orientated in <110> directions. The curved step edges are typically much smaller than the other and therefore have only very weak contrast in the topographic image. Illumination in the presence of aqueous $AgNO_3$ causes silver to deposit on only some of the terraces (see Fig. 4(b)). Note that the unreactive terraces comprise a minority fraction of the total surface area. The lead oxidation reaction was performed on another crystal prepared in the same way and the results are shown in Fig. 4(c). This image, which is characteristic of many areas that were examined, shows that lead oxide deposits accumulate on only a minority fraction of the terraces.

The differential reactivity of the terraces suggests the possibility that they are structurally and chemically distinct. As was the case for the (100) surface, there are two possible terminations for the (111) surface (see Fig. 5). All step heights are constrained to be $(N/2)d_{111}$, and the smallest possible spacing is $d_{111}/2$ = 1.12 Å. Again, steps with odd-*N* heights separate terraces with different terminations and steps with even-*N* heights separate terraces with the same termination. When the step heights are measured, we find steps of both odd- and even-*N*, and this indicates that both the positively charged

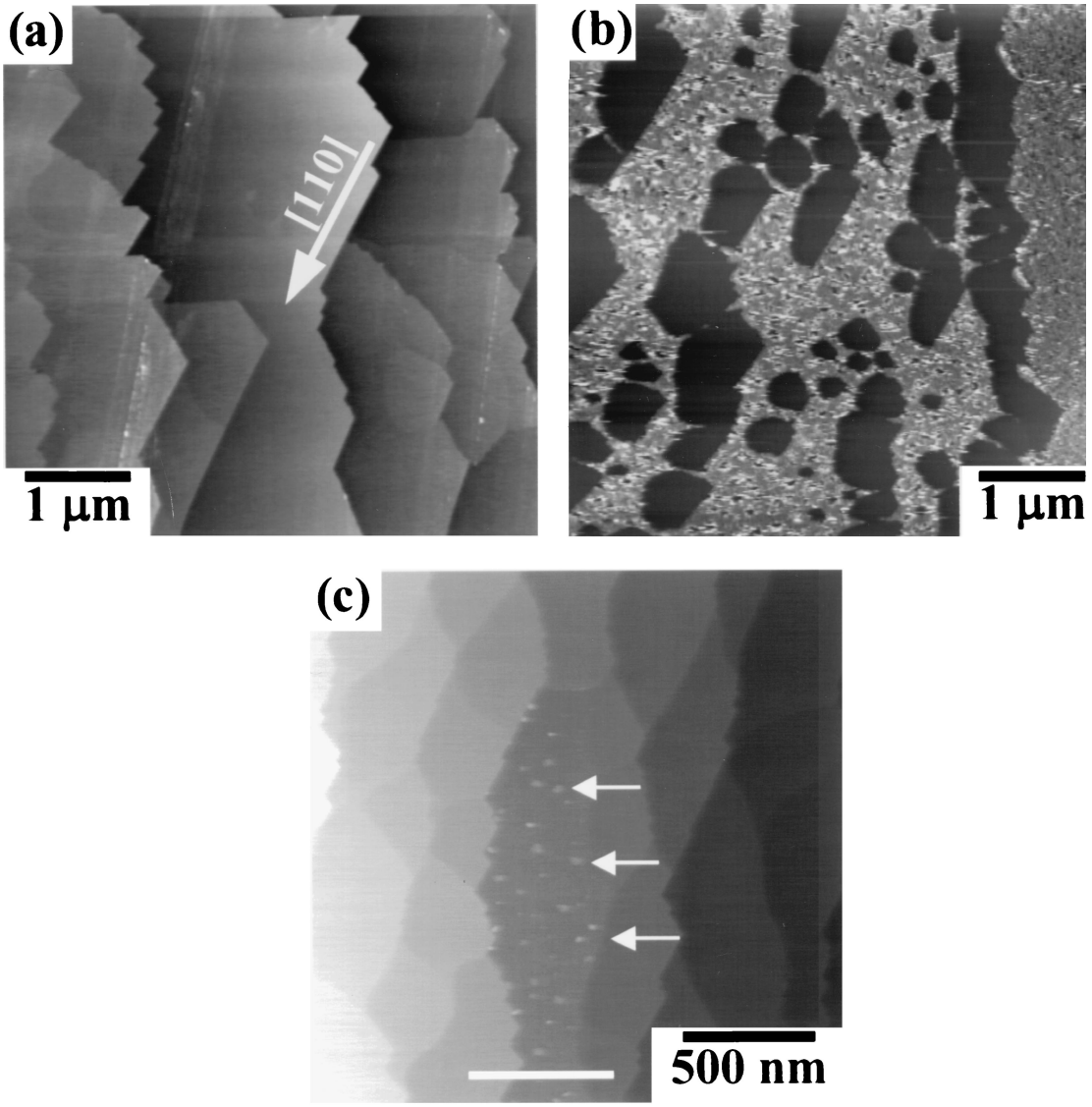

Fig. 4. Topographic AFM images of the surfaces of (111) -oriented $SrTiO_3$ single crystals. (a) Before the reactions. (b) The same surface after illumination in an aqueous $AgNO_3$ solution. The white contrast corresponds to silver. (c) a different surface after illumination in an aqueous lead acetate solution. The white contrast corresponds to lead oxide deposits. The white line indicates where the data in Fig. 6 is located. The ranges of the vertical black-to-white contrast in (a) to (c) are 60 nm, 200 nm, and 60 nm, respectively.

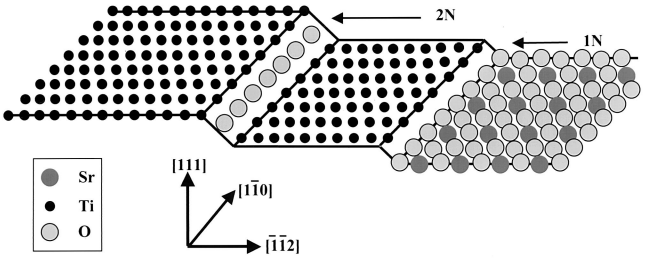

Fig. 5. Schematic drawing of the possible $SrTiO_3$ (111) surface terminations. The left terrace has a Ti^{4+} termination. Traversing an even-*N* step does not change the chemical termination while traversing an odd-*N* step changes the chemical termination to SrO_3^{4-} (right terrace). Note that the step edges are {100} type. Layer spacing (N) = $\sqrt{3}a/6$ = 1.12 Å.

titanium terminated surface and the negatively charged SrO_3 surface are simultaneously present on the $SrTiO_3$(111) surface.

To test the idea that each type of reaction was limited to terraces with the same termination, we correlated the reactivity of the terrace with the heights of its bounding steps. For example, Fig. 6 shows a sample line scan from Fig. 4(c), along the line indicated in the topograph. The height measurements can be used to differentiate steps separating terraces of constant termination from terraces with different terminations. We find that the steps that change the terrace termination separate the active and inactive terraces. Conversely, steps that preserve the termination separate terraces that have the same reactivity. The same phenomenon was observed for the silver reduction reaction.

Because the silver reduction and lead oxidation reactions were not performed on the same crystal (removing the deposits after the first reaction irreversibly changed the surface), it is impossible to be sure that the reactions are taking place on different terraces. However, because there is a consistent difference in surface area between terraces that accumulate silver and those that accumulate lead oxide, it is likely that these photochemical reactions take place on complementary terraces.

The AFM topograph in Fig. 7(a) shows an annealed $SrTiO_3$(110) surface. The surface consists of (110) terraces with straight step edges; the long steps are along <100>. A previous UHV STM study concluded that after repeated annealing >1000°C, the (110) surface is a reconstructed SrTiO termination composed of {100}-type microfacets.[21] The current observations provide no evidence for the existence of microfacets on this surface, and we attribute this to the difference in the preparation conditions (temperature and partial pressure of oxygen). The image in Fig. 7(b) is a NC-AFM topograph of this surface after illumination in the presence of aqueous $AgNO_3$. In this case, we see that the white contrast (silver) has accumulated only along the step edges. The lead oxidation reaction was performed on another crystal prepared

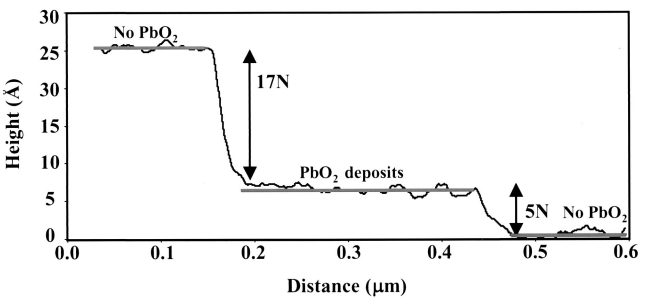

Fig. 6. Height profile on the $SrTiO_3$ (111) surface (see white line in Fig. 4(c)) showing how the change in reactivity is related to a change in chemical termination. The terrace in the middle contains PbO_2 deposits, whereas the adjacent terraces do not. The left and middle terraces are separated by a step of ~17*N* (19.4 Å) and the middle and right terraces are separated by a step of ~3*N* (5.42 Å).

in the same way, and the results are shown in Fig. 7(c). This image shows that large lead oxide deposits occur, widely spaced, along the step edges and smaller lead oxide deposits accumulate on certain terraces; other terraces are nearly free of the oxidized products. The (110) surface can also be terminated by two different and oppositely charged polar layers, as illustrated in Fig. 8. As with the (111) surface, step height measurements indicate that termination-preserving steps separate terraces with the same reactivity, whereas termination-changing steps separate terraces with different reactivities (see Fig. 9).

IV. Discussion

To begin a discussion of the observations, we note that the probe reactions used in this study reveal only the reduction and oxidation half of each of two different photochemical reactions that are not expected to have the same rate. Therefore, it is not meaningful to compare the amount of oxidized lead to the amount of reduced silver deposited on a certain surface. In all cases, the lead oxidation is slower, but that does not imply that oxidation itself is slower. In fact, charge neutrality requires that for each reaction, the reduction and oxidation occur at equal rates. For the reduction of silver, the complementary reaction is the oxidation of water and, for the oxidation of lead, the complementary reaction is the reduction of O_2; either of these "invisible" reactions may, in fact, be the rate-limiting step. Therefore, each probe reaction measures only the overall reaction rate and indicates the location at which one of two half reactions occurs.

The observations indicate that the relative photochemical reactivities of $SrTiO_3$ surfaces depend on both the crystallographic orientation of the surface and, in the case of the polar surfaces, the composition of the atomic termination layer. Three orientations were examined and, by assuming bulk terminations, two distinct surface chemistries can be identified for each orientation. Therefore, there are six distinct possible surfaces. The observed step heights indicate that after the 1200°C anneal in air, both possible terminations coexist on all three orientations. Our observations show that the nonpolar (100) surface is the most reactive. In this case, there is no evidence that the reactivity depends on the composition of the termination layer. On the other hand, for the polar (110) and (111) surfaces, terraces with distinct terminations do have different reactivities. These observations are discussed in more detail below in terms of what is already known, or can be reliably inferred about the $SrTiO_3$ surfaces.

As mentioned earlier and illustrated in Fig. 3, the (100) surface of $SrTiO_3$ can be terminated by either a TiO_2 layer or by a SrO layer. Because calculated energies for these two terminations differed by only 0.2 J/m^2, Mackrodt[22] predicted that both terminations would coexist, and this has proved to be the case.[20] Recent studies of the $SrTiO_3$ (100) surface composition conclude that the titanium-rich surface is more stable.[20,23–27] In two of these cases, it was concluded that the surface is composed of TiO_2 with disordered strontium adatoms;[24,25] however, the preparation of these surfaces (vacuum annealing) was so completely different from ours that the relevance to the present situation is questionable.

Even though step height measurements demonstrate the coexistence of SrO and TiO_2 terminated terraces, there was no sign of spatially selective reactions; this distinguishes the (100) surface from the (110)- and (111)-oriented surfaces. In this context, it is worth noting that this is the only one of the three orientations that is terminated by charge neutral layers. Furthermore, the uniform coverage of reduced silver on $SrTiO_3$ (100) is similar to observations on the TiO_2(101), which is the most reactive surface of rutile.[11] Although both the TiO_2 terminated $SrTiO_3$ (100) surface and the TiO_2(101) surface reveal five-coordinate titanium atoms, the apparent equivalent reactivity of the SrO terminated terraces suggests that the details of the atomic structure on the surface might not be the deciding factor. The terrace termination also has no apparent influence the oxidation reaction, which leaves products dispersed at widely separated positions on this surface. The

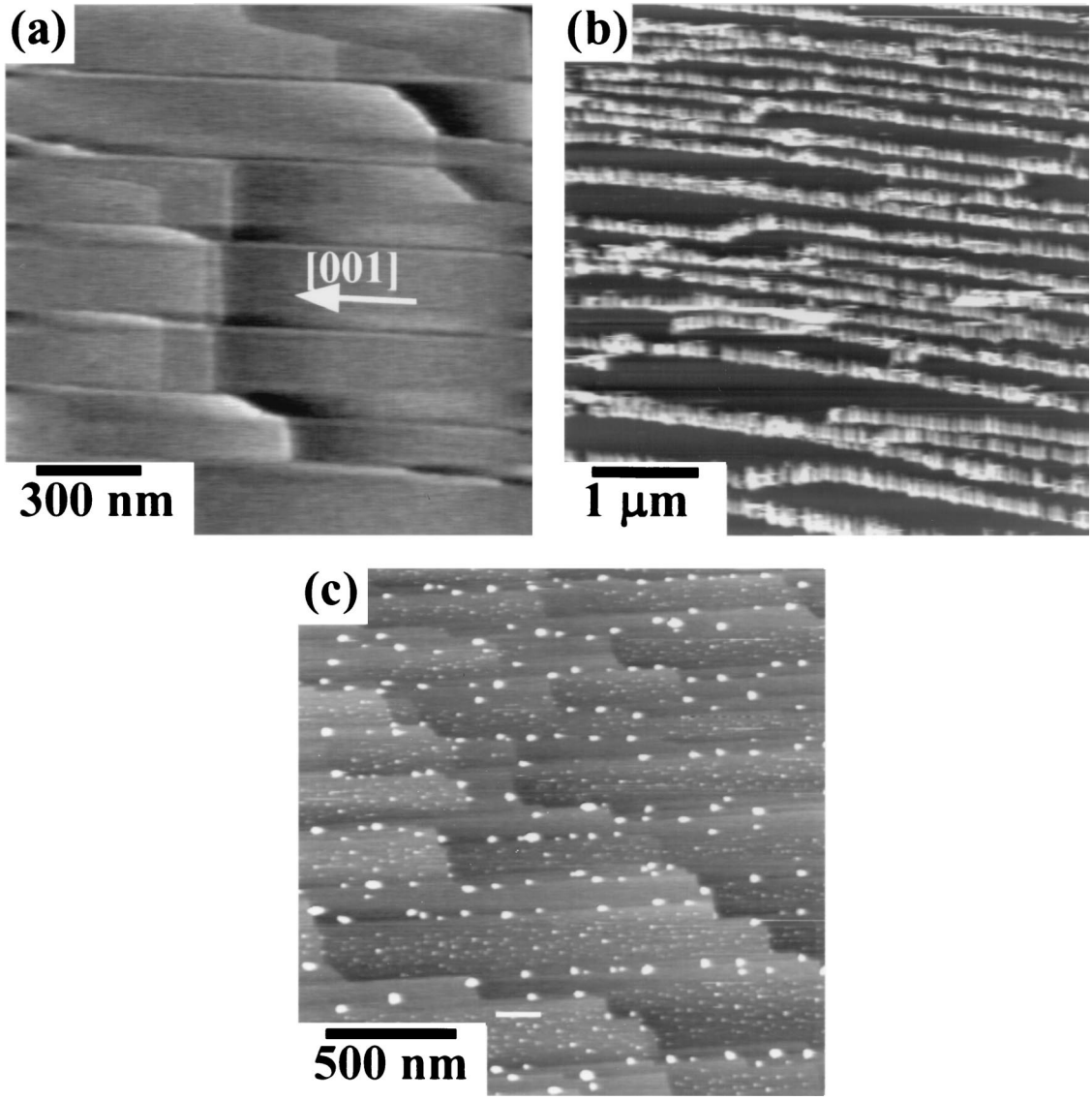

Fig. 7. Topographic AFM images of the surfaces of (110)-oriented $SrTiO_3$ single crystals: (a) before the reactions. (b) NC-AFM topograph of same surface after illumination in an aqueous $AgNO_3$ solution. The white contrast corresponds to silver. (c) A different surface after illumination in an aqueous lead acetate solution. The white contrast corresponds to lead oxide deposits. The white line indicates where the data in Fig. 9 is located. The ranges of the vertical black-to-white contrast in (a)–(c) are 30 nm, 300 nm, and 35 nm, respectively.

sparse distribution of products might arise if the reaction (or even the precipitation of the PbO_2) is initiated by defect sites not resolved in the images.

The idealized model of charge neutral SrO and TiO_2 terraces does not seem consistent with the relatively uniform photochemical properties of the $SrTiO_3$(100) surface. One possibility that the surface is actually chemically more uniform than expected from the ideal bulk termination model. For example, one study of UHV annealed surfaces indicated more uniform titanium-rich terminations.[23] The assumption that these nonpolar layers are charge neutral might also be overly simplistic. Calculations have shown that these "nonpolar" surfaces can actually possess a nonzero dipole moment perpendicular to the surface that results from incomplete charge transfer from the metals to the oxygen, or different vertical relaxations of the surface ions.[28,29] Goniakowski and Noguera[28] refer to such surfaces as "weakly polar." Although a uniform dipolar field would be consistent with the present observations, the calculations do not agree on the sign or magnitude of the polarization.

In contrast to the (100) surface, the reaction products observed on the (111) surface are selectively deposited on specific terraces. As illustrated in Fig. 5, the (111) surface can be terminated by a positively charged titanium layer or a negatively charged SrO_3

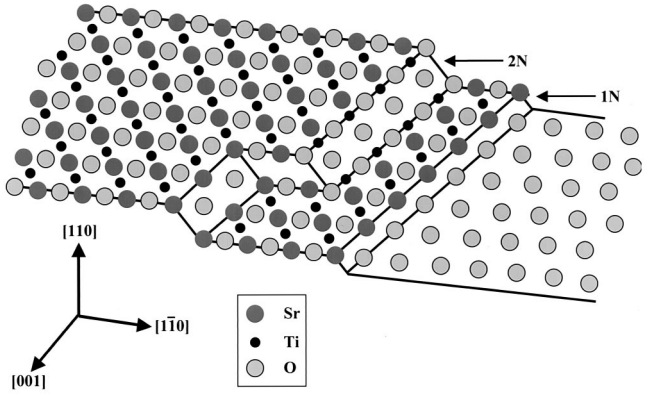

Fig. 8. Schematic drawing of the $SrTiO_3$ (110) surface terminations. The left terrace has a $SrTiO^{4+}$ termination. Traversing an even-*N* step does not change the chemical termination while traversing an odd-*N* step changes the chemical termination to O_2^{4-} (right hand terrace). Note that the step edges are {100} type. Layer spacing = $\sqrt{2}a/4$ = 1.38 Å.

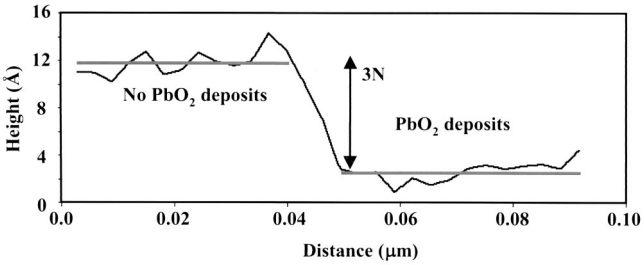

Fig. 9. Height profile on the $SrTiO_3$ (110) surface (see white line in Fig. 7(c)) showing how the change in reactivity is related to a change in chemical termination. The terrace on the left contains PbO_2 deposits and is separated by a step of $\sim 3N$ (4.3 Å) from a terrace without PbO_2 deposits.

layer; the step height measurements indicate the simultaneous presence of these terminations and the accumulation of products on terraces of the same character. The observation that the terraces that are inert for reduction comprise a minority fraction of the total area, and are comparable in area to the terraces that are active for oxidation, suggests that the reduction and oxidation products accumulate on terraces with complementary charges. Previous studies of the $SrTiO_3$(111) surface indicate that the surface has a higher concentration of titanium than Strontium.[30–32] These reports are consistent with the simultaneous presence of the titanium and SrO_3 terraces, with the titanium termination being predominant. Assuming this to be the case on the surfaces that we have examined, then the terraces that promote reduction are the predominant, positively charged, titanium-terminated terraces and the terraces that promote oxidation are the negatively charged SrO_3 surfaces.

This assignment, which is difficult to experimentally confirm, would be entirely consistent with the previous observations of $BaTiO_3$.[12,13] In the case of $BaTiO_3$, the domains with the positive ends of dipoles on the surface promoted reduction and domains with dipoles in the opposite direction promoted oxidation. The likely mechanism for this selective reactivity is that that dipolar fields drive electrons to positively charged surfaces and holes to negatively charged surfaces. This same explanation can be applied to the $SrTiO_3$(111) surface, except that in this case, the dipolar fields are created by charged surface termination layers.

The reactivity of the $SrTiO_3$(110) surface also shows a strong surface structure sensitivity and that polar surface terminations are responsible for the accumulation of oxidation products on some but not all terraces. As illustrated in Fig. 8, the surface can be terminated by an oxygen layer with a negative charge or by a SrTiO layer with a positive charge. From the current data, it is not possible to determine which of these is responsible for the oxidation reaction. However, by analogy with the $BaTiO_3$ observations, the negatively charged oxygen terrace is the likely candidate. It should also be noted that all the (110) terraces are apparently inert for reduction. The reduction products instead accumulate only on the step edges. Oxidation products are also found both on step edges and (110) terraces, but with different morphologies; they are larger and more widely dispersed on the step edges.

The reactivity of the inclined portion of the steps is easily explained if they have the (100) orientation. Based on the directions of the steps, we know that the orientation of the inclined portion of the surface is in the <100> zone. Because these steps are only a few Å high, the most likely orientation is (100), as illustrated in Fig. 8. Therefore, the extensive silver reduction that occurs on these steps is entirely consistent with observations of silver reduction on the (100) surface. Moreover, oxidation products dispersed along the steps at irregular intervals are also consistent with observations on the (100) surface. Considering the fact that the majority of the reaction products accumulate at step sites, the ideal (110) surface is the least reactive of the orientations that have been examined.

V. Conclusions

The photochemical properties of $SrTiO_3$ depend on both the crystallographic orientation of the surface and the composition of the atomic termination layer. The charge neutral (100) surface is the most reactive, the (110) surface is the least reactive, and the (111) surface has an intermediate reactivity. Two different surface terminations coexist on each of the low index surfaces. No difference in the reactivity of the two (100) terminations was observed. However, on the polar (111) and (110) surfaces, the reduction and oxidation reactions occur on terraces with different terminations and opposite charges; this leads to a nonuniform distribution of reaction products. These observations lead us to conclude that dipolar fields arising from surface domains with uniform polar terminations influence the transport of photogenerated electrons and holes and promote spatially selective oxidation and reduction reactions.

References

[1]S. P. Pappas and R. M. Fischer, "Photo-Chemistry of Pigments: Studies on the Mechanism of Chalking," *J. Paint Technol.*, **46** [599] 65–72 (1974).

[2]H. G. Völz, G. Kaempf, H. G. Fitzky, and A. Klaeren, "The Chemical Nature of Chalking in the Presence of Titanium Dioxide Pigments"; pp. 163–82 in *Photodegradation and Photostabilization of Coatings*. Edited by S. P. Pappas and F. H. Winslow. American Chemical Society, Washington D.C., 1981.

[3]G. Irick Jr., G. C. Newland, and R. H. S. Wang, "Effect of Metal Salts on the Photoactivity of Titanium Dioxide"; pp. 147–62 in *Photodegradation and Photostabilization of Coatings.* Edited by S. P. Pappas and F. H. Winslow. American Chemical Society, Washington D.C., 1981.

[4]D. F. Ollis, "Contaminant Degradation in Water," *Environ. Sci. Technol.*, **19** [6] 480–84 (1985).

[5]D. F. Ollis, E. Pelizzetti, and N. Serpone, "Photocatalyzed Destruction of Water Contaminants," *Environ. Sci. Technol.*, **25** [9] 1522–29 (1991).

[6]D. Blake, "Solar Photocatalytic Detoxification of Water"; p. 167 in *Advances in Solar Energy*, Vol. 7. Edited by K. W. Böer. American Solar Energy Society, Boulder, CO, 1992.

[7]A. Fujishima, K. Hashimoto, and T. Watanabe, *TiO_2 Photocatalysis: Fundamentals and Appplications.* BKC, Inc., Tokyo, Japan, 1999 (English translation).

[8]A. J. Bard, "Design of Semiconductor Photoelectrochemical Systems for Solar Energy Conversion," *J. Phys. Chem.*, **86** [2] 172–77 (1982).

[9]R. Memming, "Photoelectrochemical Solar Energy Conversion"; pp. 81–112 in *Electrochemistry II*. Edited by E. Steckhan. Springer-Verlag, Berlin, 1988.

[10]P. A. Morris Hotsenpiller, J. D. Bolt, W. E. Farneth, J. B. Lowekamp, and G. S. Rohrer, "The Orientation Dependence of Photochemical Reactions on TiO_2 Surfaces," *J. Phys. Chem*, **B102** [17] 3216–26 (1998).

[11]J. B. Lowekamp, G. S. Rohrer, P. A. Morris Hotsenpiller, J. D. Bolt, and W. D. Farneth, "Anisotropic Photochemical Reactivity of Bulk TiO_2 Crystals," *J. Phys. Chem.*, **B102** [38] 7323–27 (1998).

[12]J. L. Giocondi and G. S. Rohrer, "Spatially Selective Photochemical Reduction of Silver on the Surface of Ferroelectric Barium Titanate," *Chem. Mater.*, **13** [2] 241–42 (2001).

[13]J. L. Giocondi and G. S. Rohrer, "Spatial Separation of Photochemical Oxidation and Reduction Reactions on the Surface of Ferroelectric Barium Titanate," *J. Phys. Chem.*, **B105** [35] 8275–77 (2001).

[14]K. L. Kliewer and J. S. Koehler, "Space Charge in Ionic Crystals: I, General Approach with Application to NaCl," *Phys. Rev. A*, **140** [4A] A1226–40 (1965); R. B. Poeppel and J. M. Blakely, "Origin of Equilibrium Space Charge Potentials in Ionic Systems," *Surf. Sci.*, **15** [3] 507–23 (1969).

[15]P. W. Tasker, "The Stability of Ionic Crystals," *J. Phys. C: Solid State Phys.*, **12** [22] 4977–84 (1979).

[16]W. C. Clark and A. G. Vondjidis, "Infrared Study of the Photocatalytic Reaction between Titanium Dioxide and Silver Nitrate," *J. Catal.*, **4** [6] 691–96 (1965).

[17]J.-M. Herrmann, J. Disdier, and P. Pichat, "Photocatalytic Deposition of Silver on Powder Titania: Consequences for the Recovery of Silver," *J. Catalysis.*, **113** [1] 72–81 (1988).

[18]K. Tanaka, K. Harada, and S. Murata, "Photocatalytic Deposition of Metal Ions onto Titanium Dioxide Powder," *Sol. Energy*, **36** [2] 159–61 (1986).

[19]J. Torres and S. Cervera-March, "Kinetics of the Photoassisted Catalytic Oxidation of Lead(II) in Titania Suspensions," *Chem. Eng. Sci.*, **47** [15–16] 3857–62 (1992).

[20]G. Koster, B. L. Kropman, J. H. M. Rijnders, and D. H. A. Blank, "Quasi-ideal Strontium Titanate Crystal Surfaces through Formation of Strontium Hydroxide," *Appl. Phys. Lett.*, **73** [20] 2920–22 (1998).

[21]H. Bando, Y. Aiura, Y. Haruyama, T. Shimizu, and Y. Nishihara, "Structure and Electronic States on Reduced $SrTiO_3$ (110) Surface Observed by Scanning Tunneling Microscopy and Spectroscopy," *J. Vac. Sci. Technol. B.*, **13** [3] 1150–54 (1995).

[22]W. C. Mackrodt, "Atomistic Simulations of Oxide Surfaces," *Phys. Chem. Miner.*, **15** [3] 228–37 (1988).

[23]Q. D. Jiang and J. Zegenhagen, "c(6 × 2) and c(4 × 2) Reconstruction of $SrTiO_3$(001)," *Surf. Sci.*, **425** [2–3] 343–54 (1999).

[24]T. Kubo and H. Nozoye, "Surface Structure of $SrTiO_3$(100)–(Ö5 ′ Ö5)–R26.6°," *Phys. Rev. Lett.*, **86** [9] 1801–804 (2001).

[25]P. A. W. Van der Heide, Q. D. Jiang, Y. S. Kim, and J. W. Rabalais, "X-ray Photoelectron Spectroscopic and Ion Scattering Study of the $SrTiO_3$(001) Surface," *Surf. Sci.*, **473** [1–2] 59–70 (2001).

[26]G. Koster, G. J. H. M. Rijnders, D. H. A. Blank, and H. Rogalla, "Surface Morphology Determined by (001) Single-Crystal $SrTiO_3$ Termination," *Physica C*, **339** [4] 215–30 (2000).

[27]G. Charlton, S. Brennan, C. A. Muryn, R. McGrath, D. Norman, T. S. Turner, and G. Thorton, "Surface Relaxation of $SrTiO_3$(001)," *Surf. Sci.*, **457** [1–2] L376–80 (2000).

[28]J. Goniakowski and C. Noguera, "The Concept of Weak Polarity: An Application to the $SrTiO_3$(001) Surface," *Surf. Sci.*, **465** [2] L657–62 (1996).

[29]E. Heiffets, E. A. Kotomin, and J. Maier, "Semi-empirical Simulations of Surface Relaxation for Perovskite Titanates," *Surf. Sci.*, **462** [1–3] 19–35 (2000).

[30]S. Sekiguchi, M. Fujimoto, N.-G. Kang, S. Koizumi, S.-B. Cho, and J. Tanaka, "Structure Analysis of $SrTiO_3$ (111) Polar Surfaces," *Jpn. J. Appl. Phys.*, **37** [7] 4140–43 (1998).

[31]S. Sekiguchi, M. Fujimoto, M. Nomura, S.-B. Cho, J. Tanaka, T. Nishihara, N.-G. Kang, and H.-H. Park, "Atomic Force Microscopic Observation of $SrTiO_3$ Polar Surface," *Solid State Ionics*, **108** [1–4] 73–79 (1998).

[32]W. M. Sigmund, M. Rotov, Q. D. Jiang, J. Brunen, J. Zegenhagen, and F. Aldinger, "A Titanium-Rich (111) Surface of $SrTiO_3$ Single Crystals by Thermal Annealing," *Appl. Phys. A.*, **65** [2] 219–20 (1997). □